Large–scale rapid access holographic memory

Geoffrey W. Burr, Xin An, Fai H. Mok†, and Demetri Psaltis

Department of Electrical Engineering
California Institute of Technology, MS 116–81, Pasadena, CA 91125
†Also affiliated with Holoplex, Inc.,
600 S. Lake Avenue, Suite 102, Pasadena, CA 91106
e-mail: goffbo,axin,fai,psaltis@sunoptics.caltech.edu

ABSTRACT

We describe a page–formatted random–access holographic memory capable of storing up to 160,000 holograms. A segmented mirror array allows a 2–dimensional angle scanner to provide access to any of the stored holograms. High–speed random access can be achieved with a non–mechanical angle scanner. We demonstrate holographic storage and high–speed retrieval using an acousto–optic deflector (AOD).

1 INTRODUCTION

In volume holographic memories data is stored in the interference patterns formed by coherent beams of light. The information is imprinted on one of these beams (object beam). Multiple pages of data can be superimposed within the same volume of a storage medium. These pages, stored as separate holograms, can be independently accessed by changing either the angle,[1] wavelength[2,3] or phase code[4,5] of the reference (non–information–bearing) beam. The storage capacity C achievable with each of these methods can be written as $C = NM$, where N is the number of bits in each stored page, and M is the number of pages superimposed in the same volume. Assuming one bit per pixel, current spatial light modulator (SLM) technology can provide 10^5—10^6 bits per stored page. Because these pixels are recalled in parallel by a single reference beam, very high data rates can be achieved.

We describe a holographic data storage system in which the data rate is limited only by the material dynamic range. By using the 90° interaction geometry, we have enough distinct reference angles for storage of 10,000 holograms at a single location. A segmented mirror array enables non–mechanical scanners to provide high–speed random access to any of 160,000 holograms. We demonstrate holographic storage using a non–mechanical, acoustic–optic deflector. We characterize system performance by analyzing the signal-to-noise ratio (SNR) of reconstructed holograms.

0-8194-1873-0/95/$6.00

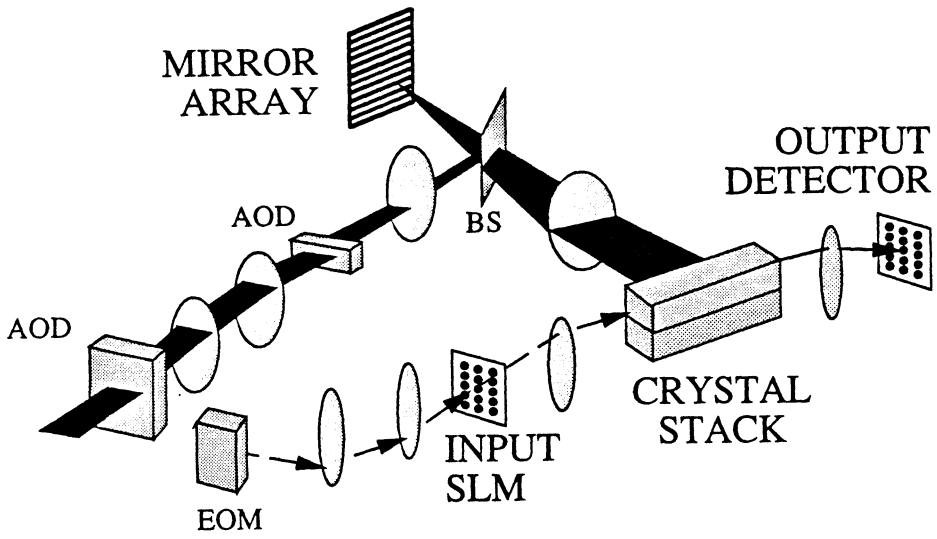

Figure 1: diagram of 160,000 hologram memory system.

2 160,000 HOLOGRAM SYSTEM

The system design is shown in Figure 1. A laser beam is split in two parts and then brought together at a storage location within a stack of photorefractive crystals. Information is imprinted on the object using a spatial light modulator (SLM), while the reference beam contains no information. A segmented mirror array and two crossed acousto–optic deflectors (AODs) allow the reference arm of the system to control both the position and angle of incidence of this reference beam. Another AOD is used to deflect the object beam to control the position of the information-bearing object beam on the crystals. The Doppler shift introduced by the AODs is compensated in the object arm by an electro–optic modulator (EOM) so that the interference pattern is stationary during storage. In order to store 160,000 holograms, we need 16 different positions on the crystals where we can store 10,000 holograms each. Any of the 160,000 stored pages can be accessed randomly in approximately 100 μsec. With 1000 $\times$ 1000 pixel SLMs, this yields a total storage of 160Gbits and a readout rate of 10 Gbits/sec.

The key element in our realization of angle and spatial multiplexing is the segmented mirror array, which preserves horizontal angular multiplexing while using vertical deflection to step between distinct storage locations. In the next section, we describe the operation of such a mirror array.

3 SEGMENTED MIRROR ARRAY

Figures 2a and 2b diagram the operation of the mirror array—Figure 2a shows selection of output location by the vertical angle scanner (AOD), while Figure 2b shows angle multiplexing at a spot by the horizontal AOD. The deflection angle of the vertical AOD determines which mirror strip will be illuminated. By tilting each mirror strip at different angles, we can address different locations on the crystals. The mirror strips are stacked in the vertical direction but extend horizontally, so the horizontal AOD moves the focused spot along the same mirror

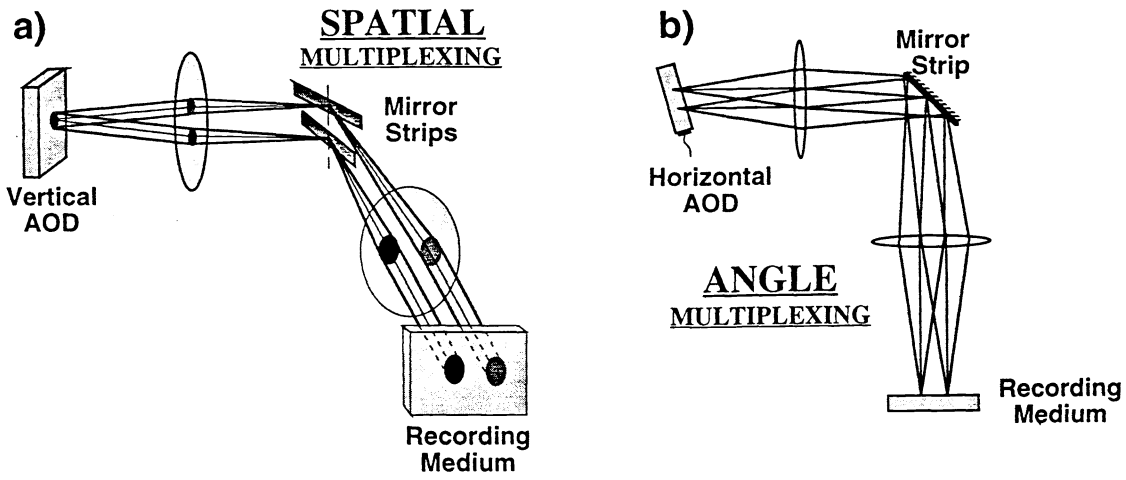

Figure 2: Control of beam location and angle using a mirror array: a) spatial multiplexing, b) angle multiplexing.

strip. The motion of the focused spot in the Fourier plane of the output lens results in a change of horizontal incidence angle at the crystal, without any motion of the spot itself. In summary, the horizontal AOD provides angle multiplexing at any given location, while the vertical AOD selects which location is to be illuminated.

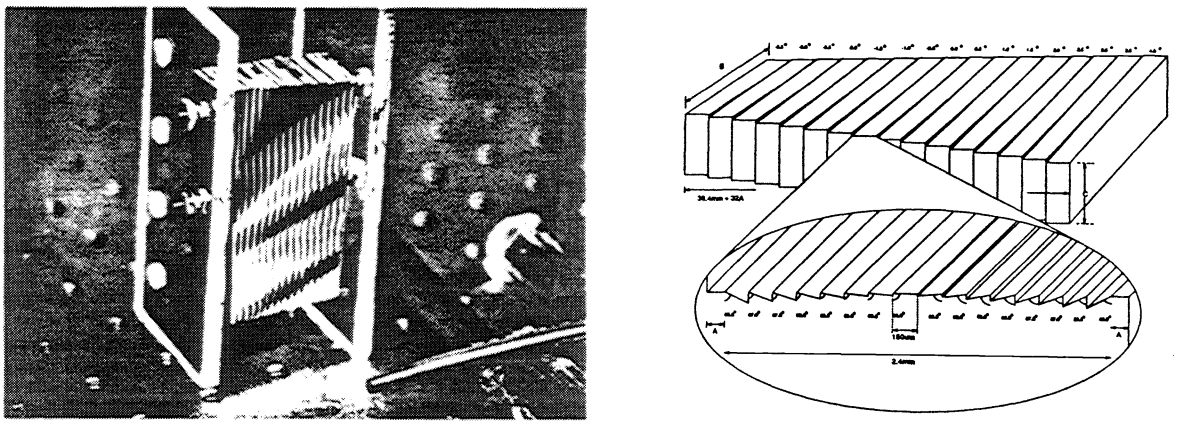

Figure 3: Segmented mirror array: a) picture, b) schematic.

The drawings show the mirror strips at 45° to the incoming beam because the operation of the mirror array is easier to explain this way. In the actual implementation (shown in Figure 3), a beamsplitter is required because the surface of the mirror array must be aligned with the focal plane (the center of the 4–F system directing the reference beam to the crystal), in which the converging beams achieve their focus. This allows us to minimize the vertical size of each mirror strip that is necessary to avoid crosstalk to other storage locations.

A prototype mirror array was constructed with blazed grating technology. This technique involves using a diamond tip to cut grooves on suitable substrates. The groove angles (0.5° step between each) are accurately controlled by the tilt of the diamond tip with respect to the substrate. The width of each groove is set to 150μm by the dimensions of the diamond itself. Each mirror strip is 75mm long. A photograph of the completed mirror array is shown in Figure 3.

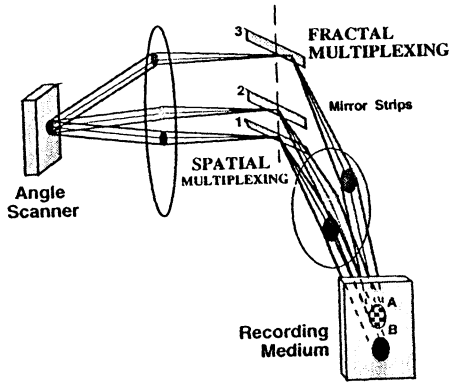

Figure 4: Fractal multiplexing, spatial multiplexing shown for comparison.

4 FRACTAL MULTIPLEXING

Since current AOD technology can provide SBP on the order of 1000 or so, storage of up to 10000 holograms at each location of the above system is problematic. The horizontal AOD is overloaded by the large number of angles required, while the vertical AOD is underutilized. Our solution is to use multiple mirror facets for each location, reducing the number of angularly multiplexed holograms required per facet. This can be accomplished using fractal multiplexing, as shown in Figure 4.

Normal angle–multiplexing relies on Bragg–mismatch: that is, very small changes in horizontal incidence angle can make the output disappear. In contrast, a change in vertical incidence angle will not cause Bragg mismatch, but only a commensurate change in the angle along which the output image is reconstructed. If this output angle becomes larger than the vertical angular bandwidth of the image, the reconstruction of the hologram is completely displaced off the output detector. At this point, the reference beam can be used to store and independently recall another hologram whose reconstruction falls directly on the original detector. Note that these reference beams reconstruct multiple holograms—but only one of the stored pages hits the output detector. This out-of-plane multiplexing was originally conceived in terms of finding non–degenerate 2–D to 2–D interconnection schemes, and the fractal name arose from the scale invariance which these patterns share.[6] Later, fractal multiplexing was used to store 5000 holograms at a single location.[7]

5 STORAGE OF 10,000 HOLOGRAMS

In this section, we describe an experiment combining the LILA architecture with fractal multiplexing and the mirror array. Figure 5 shows the experimental setup. In this setup, the mirror array delivered reference beams which were wide enough to cover the side of a crystal bar. The reference arm contained an XY mechanical scanner which moved the focused reference beam across the surface of the mirror array, horizontal for angle multiplexing, vertical for fractal and spatial multiplexing. Not shown in the drawing are two cylindrical lenses which magnified the horizontal dimension of the reference beam, and two mirrors in a periscope arrangement which conveyed this beam onto the mechanical scanner. A 2 inch polarizing beamsplitter cube and quarter waveplate were used to increase the efficiency of the reference arm. The reference beam spot size was elliptical, about 20mm in width by 6mm in height.

The object beam was directed to the proper location after the image information was already been imposed on the beam. The image presented on the SLM is demagnified by 3× and deflected by a 2–D angle deflector.

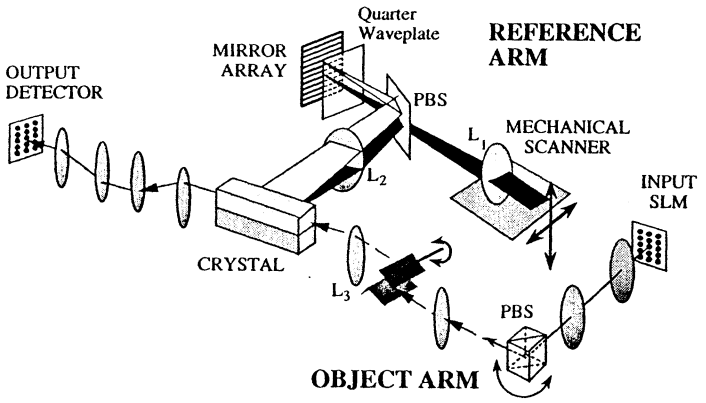

Figure 5: Experimental setup for storage of 10,000 holograms.

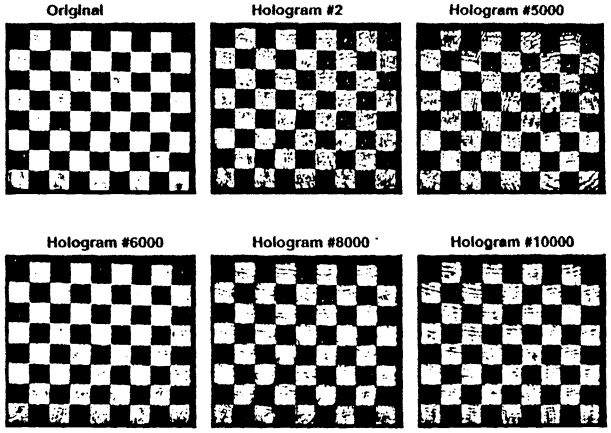

Figure 6: Reconstructions from 10,000 holograms.

On the far side of lens L_3, this deflection determined where the Fourier transform of the displayed information arrived. Since we did not use a random phase diffuser, the crystal had to be placed not exactly at the Fourier transform plane, but had to be displaced beyond it by 80mm. At the crystal location, the DC portion of the expanding image was approximately 1.8mm high $\times$ 2.4mm wide. Three lenses after the crystal provide filtering and slight magnification, and imaged the reconstructed holograms onto a Photometrics Star I cooled scientific CCD. The advantage of Fourier transform storage becomes apparent at this point, since the reconstructions from all the spatially multiplexed locations can be imaged onto a single detector array.

10,000 holograms were stored in a 0.01% Fe–doped crystal bar of dimensions $10\times10\times20$ mm. The **c**–axis was at 45° to the vertical faces. The images were displayed in text mode (80 column by 24 rows) on a 640×480 pixel VGA monitor, and sampled for the 480×440 pixel SLM. Both random bit patterns and a standard chessboard pattern were stored. The last exposure time was 0.1 second and the erasure time constant was 1200 seconds. The initial exposure lasted 0.6 seconds and the total exposure time was 35.8 minutes. Four mirror strips were used for storage with 2500 holograms stored on each, with an unused strip between each used strip. Several reconstructions are shown in Figure 6. The average diffraction efficiency was 5×10^{-9}. The average power in the reconstructions (which were already half dark) was 2.5 times the background scatter (measured before storage).

6 STORAGE USING ACOUSTO–OPTIC DEFLECTOR

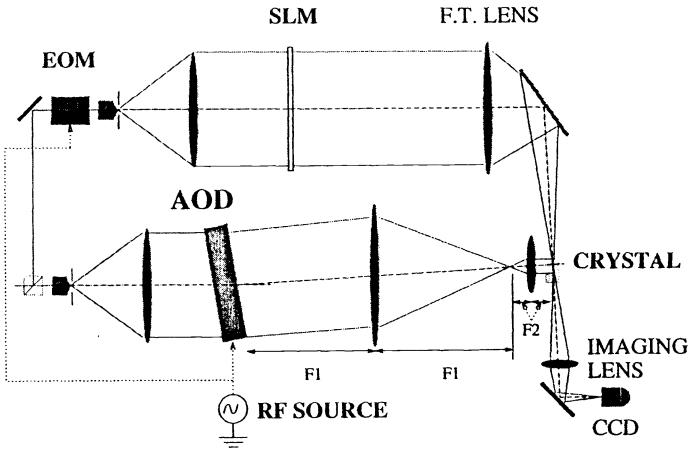

Figure 7: Storage system using AOD.

Instead of mechanical scanners, Acousto-Optic devices (AOD's) can be used to perform the angular scanning of the reference beam. AOD's have several advantages over mechanical scanners such as rapid access and accurate, repeatable setting of the reference beam angle. In a separate system, we have demonstrated storage of 500 holograms using an acousto–optic deflector to provide the horizontal reference angles, the random access time of the system is determined by the switching time of the AOD which is around 70 μsec in this case. The experimental setup is shown in Figure 7, which is similar to Figure 1, except that the mirror array and beamsplitter are not present, and only one AOD and one crystal bar was used. The SLM used was a slide, rotated by several degrees between each exposure. The reconstructed holograms were measured with a CCD array containing an 8–bit digitizer. Figure 8 shows some of the reconstructions from 500 holograms made in this system.

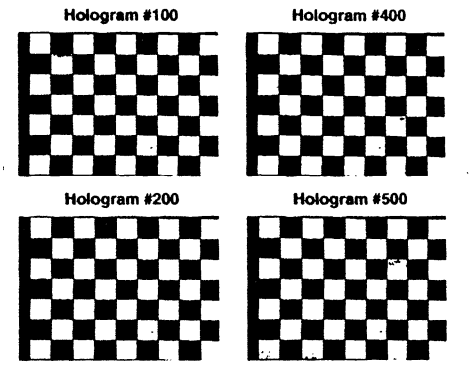

Figure 8: Reconstructions from 500 holograms.

The pixel map is divided into regions which were expected to be bright (or dark). In this process, edge pixels which were near a dark/bright transition were discarded. The two resulting histograms serve as estimates of the probability density functions (PDF) for storage of binary data. These two PDFs are shown in Figure 9 for one reconstruction—approximately 200,000 pixels from the image are represented in all. An optimal threshold can be empirically determined, giving a measured probability of error. In this experiment, 10^{-5} raw probability of

error was measured when the same threshold was used for the entire image. Using one threshold for the center portion of the image, and a different threshold for the edges, we were able to reduce this measured error to zero.

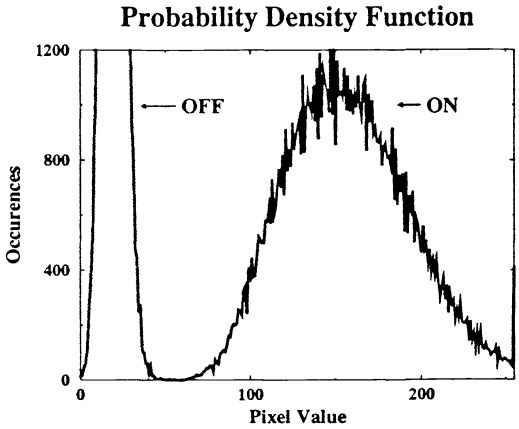

Figure 9: Histograms of OFF (dark) and ON (bright) pixels measured from one of the reconstructions.

7 NOISE CHARACTERIZATION

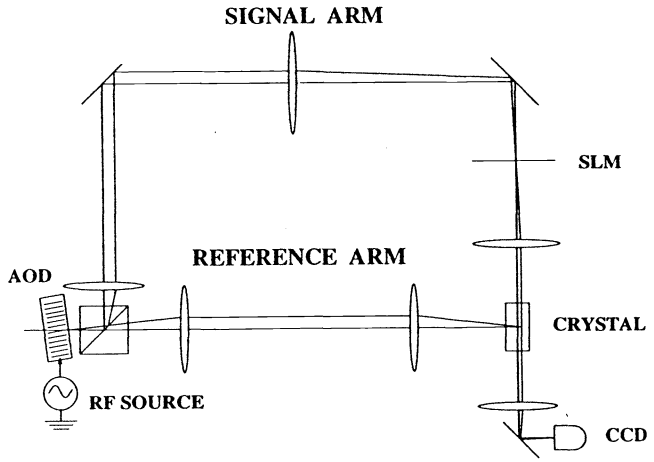

Figure 10: Single-AOD memory setup.

To characterize the noise performance in an angle multiplexed memory, we built another simple system using a single AOD. In this system, Figure 10, the AOD is used to deflect both the reference and object beams. One advantage of this architecture is that it avoids build-up of inter-pixel gratings. We used a novel method to normalize the reconstruction in order to significantly suppress deterministic sources of errors, such as beam non-uniformity and dust particles on the optical components. Since such deterministic error sources can in principle be eliminated by careful engineering, the performance we obtain through normalization provides an estimate for the performance that is expected from an optimized system. The normalized result is shown against the original reconstruction in Figure 11.

We used the following definition of signal-to-noise ratio (SNR) in order to assess the relative quality of images:

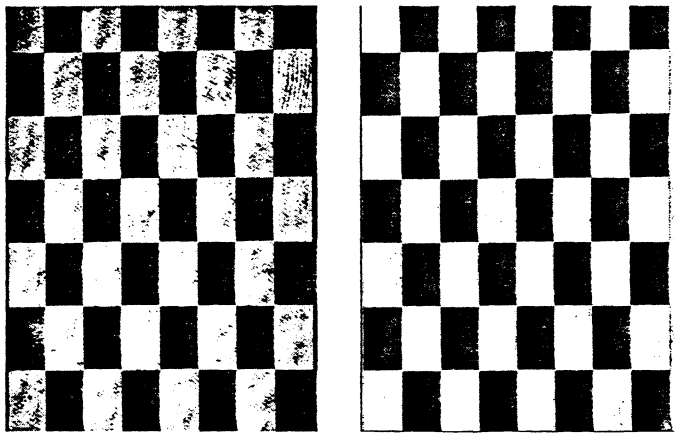

Figure 11: Original and normalized reconstruction.

$$\mathrm{SNR} = \frac{\mu_1 - \mu_0}{\sqrt{\sigma_1^2 + \sigma_0^2}}$$

where μ_0 and μ_1 are the means of the OFF and ON signals, respectively, and σ_0^2 and σ_1^2 are the corresponding variances.

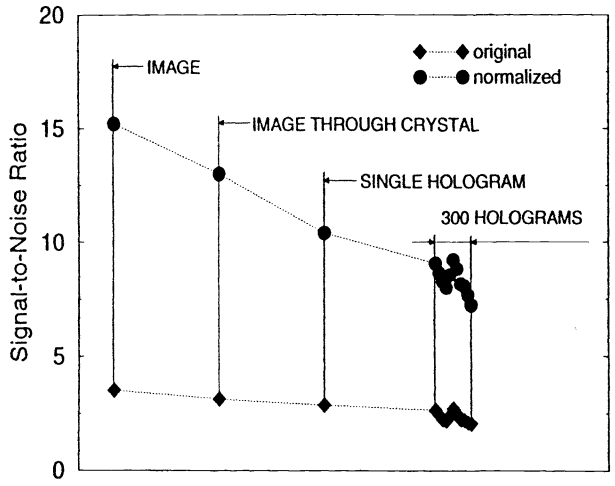

Figure 12: SNR degradation.

We performed[8] a sequence of experiments to identify the sources of SNR degradation. The result is shown in Figure 12. The normalization helps to highlight the noise sources associated with the crystal and the holographic recording. We attribute the degradation of SNR at successive experiments to the accumulation of several noise sources: multiple reflection and surface defects of the crystal; non–uniform modulation depth; scattering, fanning, crosstalk, and nonuniform erasure.

8 CONCLUSIONS

We propose an architecture of 160,000–page holographic memory. We demonstrated storage of 10,000 holograms using mechanical scanners. We achieved fast, random access to 500 stored holograms in a separate system using acousto–optic deflection. We characterized the noise performance of an angle multiplexed system. Future work will be focused on the combination of the current storage system and AOD's for the implementation of large-scale, fast random-access holographic storage.

9 ACKNOWLEDGMENTS

This work is funded by Rome Lab/IRAP under contract # 30602–94–C–0182. We thank George Barbastathis for helpful discussions and Yayun Liu for technical assistance.

10 REFERENCES

[1] D. L. Staebler, J. J. Amodei, and W. Philips. "Multiple storage of thick phase holograms in $LiNbO_3$". In *VII International Quantum Electronics Conference*, Montreal, May 1972.

[2] F. T. S. Yu, S. Wu, A. W. Mayers, and S. Rajan. "Wavelength multiplexed reflection matched spatial filters using $LiNbO_3$". *Opt. Commun.*, 81:343, 1992.

[3] G. A. Rakuljic, V. Leyva, and A. Yariv. "Optical data storage by using orthogonal wavelength–multiplexed volume holograms". *Opt. Let.*, 17:1471, 1992.

[4] T. F. Krile, M. O. Hagler, W. D. Redus, and J. F. Walkup. "Multiplex holography with chirp–modulated binary phase–coded reference–beam masks". *Appl. Opt.*, 18:52, 1979.

[5] J. E. Ford, Y. Fainman, and S. H. Lee. "Array interconnection by phase–coded optical correlation". *Opt. Let.*, 15:1088, 1990.

[6] H. Lee, X.-G. Gu, and D. Psaltis. "Volume holographic interconnections with maximal capacity and minimal cross talk". *J. Appl. Phys*, 65(6):2191–2194, March 1989.

[7] F. H. Mok. "Angle-multiplexed storage of 5000 holograms in lithium niobate". *Optics Letters*, 18(11):915–917, June 1993.

[8] X. An and D. Psaltis. "Experimental characterization of an angle–multiplexed holographic memory", submitted to: *Optics Letters.*